Electronic Supplementary Material (ESI) for Faraday Discussions.

Supporting Information

Cationic Micelles in Deep Eutectic Solvents: Effects of Solvent Composition

Iva Manasi,*[a] Stephen M. King[b] and Karen J. Edler*[c]

[a]*Department of Chemistry, University of Bath, Claverton Down, Bath BA2 7AY, UK; E-mail: im554@bath.ac.uk*

[b]*ISIS Neutron and Muon Source, Science and Technology Facilities Council, Rutherford Appleton Laboratory, Didcot OX11 0QX, UK.*

[c]*Department of Chemistry, Centre for Analysis and Synthesis (CAS) Lund University, Lund, 221 00 Sweden. Email: karen.edler@chem.lu.se*

S1 Water content measurements for the DES

The water content was measured for the 1pTSA:1ChCl, 2pTSA:1ChCl and 1pTSA:2ChCl DES as well as the DES with water, 1pTSA:1ChCl:3W and 2pTSA:1ChCl:3W, using a Karl Fisher Titrator. The titrator measures the amount of water (ppm or weight) for a certain weight of sample (DES in this case), which can then be converted to a wt% of water in the DES. The water content in wt% measured for the DES used in this study are given in the Table S1 along with the calculated theoretical values (from the the molecular weight of the constituents) and the values reported by Rodriguez et al.[1] for comparison. Our measured values are in close agreement with the theoretical values but lower than the ones measured by Rodriguez et al.

Table S1: Water content (wt%) measured for the various DES used in this study

	Theoretical water wt%	Measured water wt%	Rodriguez et al[1] water wt%
1pTSA:1ChCl	5.46	5.20	8.13
1pTSA:1ChCl:3W	18.77	16.77	
2pTSA:1ChCl	6.93	7.90	9.53
2pTSA:1ChCl:3W	15.69	16.05	
1pTSA:2ChCl	3.84	3.70	5.10

S2 Surfactant Concentration

Table S2: Table summarising the measured surfactant concentration in wt% and mM for the three DES: 1pTSA:1ChCl, 1pTSA:1ChCh:3W and 2pTSA:1ChCl:3W

	wt%	mM	wt%	mM	wt%	mM
Surfactant	1pTSA:1ChCl		1pTSA:1ChCl:3W		2pTSA:1ChCl:3W	
DTAB	2	78	2	76	2	78
DTAB	5	196	5	190	5	195
DTAB	10	392	10	380	10	391
TTAB	2	72	2	70	2	72
TTAB	5	179	5	174	5	179
TTAB	10	359	10	349	10	358
CTAB	2	66	2	64	2	66
CTAB	5	166	5	161	5	165
CTAB	10	331	10	322	10	330

S3 SLD values of various components in the system

The neutron scattering length density (SLD; ρ) of any component in a system is calculated using the equation:

$$\rho = \frac{\sum_i^n b_{c_i}}{\overline{V}}$$

where b_{c_i} is the bound coherent scattering length of atom i in a molecule and $\overline{V}$ is the volume containing all the n atoms. The volume of the 1pTSA:1ChCl DES, 1pTSA:1ChCl:3W DES and 2pTSA:1ChCl:3W DES at the HHH contrast was calculated from the physical density measured at 25 °C and the same value was used for the DDD and HDD contrast assuming that the molecular volume is independent of isotopic composition. For the surfactants the molecular volume was calculated using their molecular composition. The volumes and calculated SLD for the DES are given in Table S3 and the volumes, neutron scattering lengths and calculated SLD for various individual components in the system is given in Table S4.

Table S3: Volumes and calculated SLD of pTSA:ChCl DES at different contrasts.

DES	Contrast	Abbreviation	Density[a] g cm^{-3}	Volume Å^3	SLD $\times 10^{-06}$ Å^{-2}
1pTSA:1ChCl	H:H	110 HH DES	1.2070 ± 0.3	453.8	0.90
1pTSA:1ChCl	D:D	110 DD DES	–	453.8	2.97
1pTSA:1ChCl	H:D	110 HD DES	–	453.8	4.58
1pTSA:1ChCl:3W	H:H:H	113 HHH DES	1.1728 ± 0.2	543.6	0.66
1pTSA:1ChCl:3W	D:D:D	113 DDD DES	–	543.6	3.53
1pTSA:1ChCl:3W	H:D:D	113 HDD DES	–	543.6	4.87
2pTSA:1ChCl:3W	H:H:H	213 HHH DES	1.2040 ± 0.3	791.9	0.90
2pTSA:1ChCl:3W	D:D:D	213 DDD DES	–	791.9	2.87
2pTSA:1ChCl:3W	H:D:D	213 HDD DES	–	791.9	4.71

(a) For the DES with deuterated constituents (DDD and HDD), the molecular volume was assumed to be the same as that for the corresponding DES with hydrogenated components.

Table S4: Volumes, neutron scattering lengths ($\sum b_{c_i}$) and calculated SLD of constituents of the system. The neutron scattering length of each constituent was calculated as the sum of the neutron scattering lengths of the constituting atoms

Chemical	Formula	Volume Å^3	$\sum b_{c_i}$ fm	SLD $\times 10^{-06}$ Å^{-2}
ChCl	$C_5H_{14}NOCl$	202	5.6	0.29
d-ChCl	$C_5H_5D_9NOCl$	202	99.3	5.16
pTSA	$CH_3C_6H_4SO_3H.H_2O$	255	35.15	1.38
d-pTSA	$CD_3C_6D_4SO_3H.H_2O$	255	108.1	4.24
C_nTA$^+$ head-group[a]	$N(CH_3)_3^+$	135	-4.3	-0.3
d-C_nTA$^+$ head-group[a]	$N(CD_3)_3^+$	135	89.3	7.12
Dodecyl alkyl tail	$C_{12}H_{25}$	398.4	-14.46	-0.36
d-Dodecyl alkyl tail	$C_{12}D_{25}$	398.4	253.2	6.35
Tetradecyl alkyl tail	$C_{14}H_{29}$	453.4	-14.46	-0.39
d-Tetradecyl alkyl tail	$C_{14}D_{29}$	453.4	253.2	6.45
Hexadecyl alkyl tail	$C_{16}H_{33}$	508.4	-20.79	-0.41
d-Hexadecyl alkyl tail	$C_{16}D_{33}$	508.4	333.15	6.55

(a) The bromide will dissociate in solution and therefore the head group for the micelle is likely to comprise C_nTA$^+$.

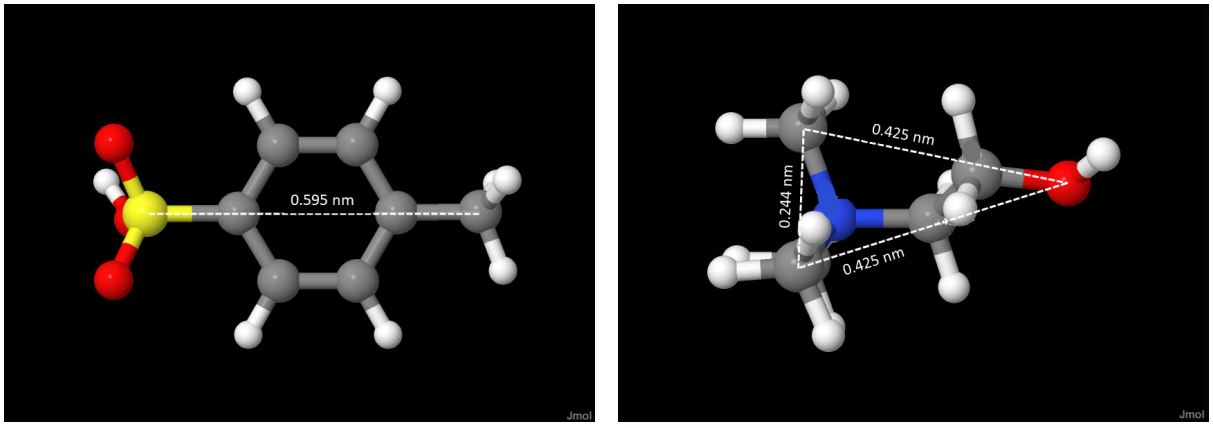

(a) (b)

Figure S1: Size of pTSA molecule (a) and choline ion (b) as measured from molecular model in Jmol.[2]

The scattered intensity, $I(q)$, of a system of monodisperse, isotropic, and centrosymmetric particles may be described by the equation:

$$I(q) = NV^2(\Delta\rho)^2 P(q)S(q)$$

where N and V are the number of particles and the volume of the particles, respectively. $\delta\rho$ is the difference between the SLD of the scatterer and the solvent. $P(q)$ refers to the form factor, which describes scattering within the particle and therefore relates to the particle shape, and $S(q)$ is the structure factor, which describes the interaction between particles in the system. Although the structure factor may be considered to be negligible at low concentrations of scatterers, at higher concentrations it is important to account for interparticle interactions, which affect the apparent scattered intensity.

S4 SANS Model Fitting

S4.1 SANS from the native DES

SANS was measured from the native DES (solvents without surfactants), as backgrounds for the subsequent studies with surfactants. The absence of features in the small angle region ($0.008 - 0.7 Å^{-1}$) suggests the solvents are unstructured on the length scale ($= 2\pi/q$) of interest to understand micellar structuring. The scattered intensity is dominated by the incoherent background scattering (primarily from 1H atoms) and is highest for the hydrogenated contrast (HHH DES) and lowest from the deuterated contrast (DDD DES).

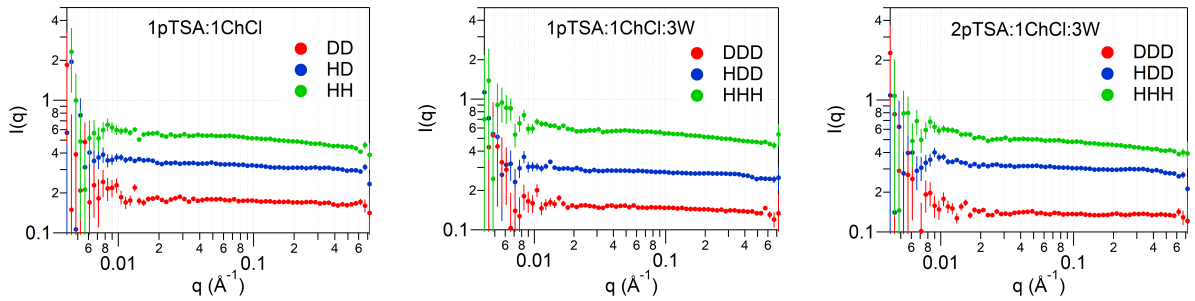

(a) (b) (c)

Figure S2: SANS measured from the native DES at 3 contrast: h-pTSA:h-ChCl:H_2O (HHH DES; green circles) h-pTSA:d-ChCl:D_2O (HDD DES; blue circles) and d-pTSA:d-ChCl:D_2O (DDD DES; red circles) at the three solvent compositions. (a) 1pTSA:1ChCl (b) 1pTSA:1ChCl:3W and (c) 2pTSA:1ChCl:3W

S4.2 Model Fitting Trials

The SANS patterns for 5 wt% DTAB, TTAB and CTAB in the three DES (1pTSA:1ChCl, 1pTSA:1ChCl:3W and 2pTSA:1ChCl:3W) were fitted to uniform spherical/ellipsoidal models and their core-shell variants to evaluate the deviations of the fits through the χ^2 parameter, which is inversely related to the quality of the fit. The models and the parameters are described in the SasView documentation [3]. The uncertainties on both the measured intensities ($I(q)$) and the derived scattering vector (q) values, which accounts for the instrumental resolution, were taken into account during the fitting. SANS from CnTAB in the solvents (Figure S3) shows scattering characteristic of globular structures such that a flat curve is observed for $q < 0.1$ Å^{-1}, which then shows a sharp decay at q-values corresponding to the length scale of the scattering particles, therefore spherical and elliptical model were considered appropriate models to fit the data. This was evaluated for 5 wt% d-CnTAB in a fully protonated DES (HHH DES) and h-CnTAB in deuterated DES (DDD DES) for all three DES; 1pTSA:1ChCl, 1pTSA:1ChCl:3W and 2pTSA:1ChCl:3W. The best fit values for the uniform spherical and uniform elliptical model parameters and the χ^2 values obtained using each model are given in Table S5. The SANS data along with the uniform spherical and uniform ellipsoidal fits and the residuals for the best fit (DTAB in 1pTSA:1ChCl DES) and the worst fit (CTAB in 1pTSA:1ChCl:3W DES) data, i.e. the lowest and highest χ^2 values, are shown in Figure S3. The residuals and the χ^2 is consistently good or bad irrespective of the model, uniform spherical or uniform elliptical.

A spherical model was ultimately chosen as no significant improvement in the fit was observed for the ellipsoidal model and there is little evidence for significant elongation in either of the data sets with x_{core}, the aspect ratio, for the ellipsoidal fits lie between 1 and 2.5 in all cases, suggesting that the micelles are spheroidal at most. The ellipsoidal fits give rather small value for the micelle radii and don't match the viscosity data, i.e. the micelles are the most elongated in the 2pTSA:1ChCl:3W DES and these micellar solutions show the lowest shear thinning behaviour and the micelles in 1pTSA:1ChCl:3W DES have the lowest x_{core} and these micellar solutions have the most shear thinning behaviour. Based on these factors, a spherical model was chosen as it as it allows for a estimation for micelle morphology while minimising the number of fit parameters and for detailed structural analysis of the micelles a spherical model or its

core-shell/core multi-shell variant were used.

Polydispersity was not required to get good fits to the data. The uncertainty in the fit parameters and the χ^2 values are small for monodisperse models, which support the decision to not include polydispersity in the models to fit the data.

Table S5: Fit parameters and χ^2 values for uniform sphere and ellipsoidal models used as potential fits for the CnTAB in all three DES; 1pTSA:1ChCl, 1pTSA:1ChCl:3W and 2pTSA:1ChCl:3W as shown in Figure S2

		Uniform sphere		Uniform Ellipsoid		
		Radius/Å	χ^2	Radius/Å	x_{core}	χ^2
				DTAB		
110 DES	d-DTAB HHH DES	10.3±0.1	1.2	6.6±0.3	2.6±0.2	1.3
	h-DTAB DDD DES		2.1			1.8
113 DES	d-DTAB HHH DES	12.5±0.1	1.7	9.7±0.2	1.9±0.1	2.4
	h-DTAB DDD-DES		2.6			2.9
213 DES	d-DTAB HHH DES	9.8±0.1	1.5	5.3±0.2	3.2±0.2	1.7
	h-DTAB DDD DES		2.4			1.7
				TTAB		
110 DES	d-TTAB HHH DES	13.0±0.1	5.6	9.6±0.2	2.1±0.1	2.9
	h-TTAB DDD DES		6.2			4.1
113 DES	d-CTAB HHH DES	15.6±0.1	8.7	14.5±0.2	1.2±0.1	9.1
	h-TTAB DDD DES		13.5			14.3
213 DES	d-TTAB HHH DES	12.0±0.1	3.5	8.5±0.2	2.2±0.1	1.7
	h-TTAB DDD DES		4.1			3.8
				CTAB		
110 DES	d-CTAB HHH DES	17.3±0.1	5.6	13.8±0.1	1.9±0.1	5.7
	h-CTAB DDD DES		5.8			4.1
113 DES	d-CTAB HHH DES	19.4±0.1	20.8	16.9±0.1	1.5±0.1	13.5
	h-CTAB DDD DES		17.2			20.8
213 DES	d-CTAB HHH DES	15.4±0.1	9.4	12.9±0.1	1.7±0.1	5.1
	h-CTAB DDD DES		4.8			7.0

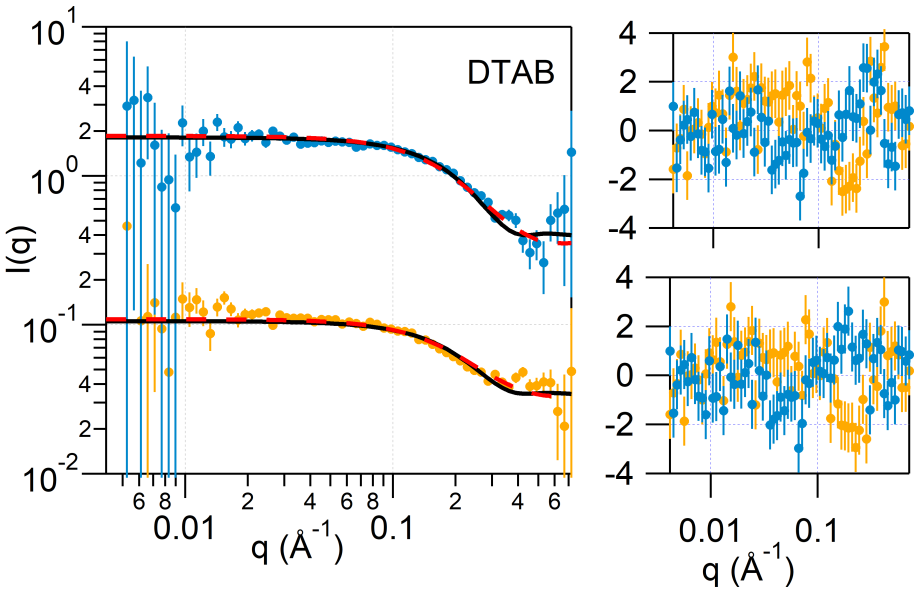

(a)

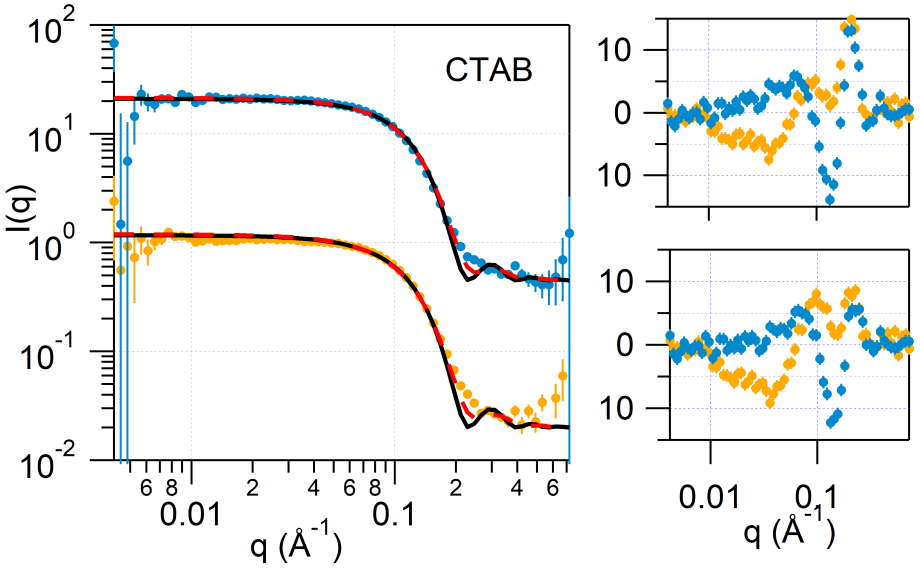

(b)

Figure S3: SANS measured from d-CnTAB in HHH DES (blue) and h-CnTAB in DDD DES (orange) contrasts for (a) 5 wt% DTAB in 1pTSA:1ChCl (least χ^2 as shown in Table S5) and (b) 5 wt% CTAB in 1pTSA:1ChCl:3W (highest χ^2 as shown in Table S5). The data were fitted to uniform sphere (black solid line) and uniform ellipsoidal (red dashed line) models. The residuals from the fits (blue for d-CnTAB in HHH DES and orange for h-CnTAB in DDD DES) are shown in the right panel with the residuals from spherical fits at the top and elliptical fits at the bottom. The SANS patterns are offset along the y-axis for clarity

S5 Results and parameters from SANS fitting

This section details the results from uniform spherical and core-shell spherical models fitted to SANS data from CnTAB in three DES.

S5.1 Concentration series of CnTAB in DES

SANS was measured for 2, 5 and 10 wt% deuterated CnTAB (DTAB, TTAB and CTAB) in the three HHH DES; 1pTSA:1ChCl, 1pTSA:1ChCl:3W and 2pTSA:1ChCl:3W. The data were fitted to a uniform spherical model with the SLD of the sphere fixed at the value for deuterated tails as shown in Table S4 (6.35×10^{-6} Å^{-2} for DTAB, 6.45×10^{-6} Å^{-2} for TTAB and 6.55×10^{-6} Å^{-2} for CTAB) and the SLD of the solvent set to the calculated value for HHH DES at the relevant composition as shown in Table S3 (0.9×10^{-6} Å^{-2} for 1pTSA:1ChCl, 0.66×10^{-6} Å^{-2} for 1pTSA:1ChCl:3W and 0.9×10^{-6} Å^{-2} for 2pTSA:1ChCl:3W). For 5 wt% CTAB and 10 wt% CnTAB in all three DES, interparticle interaction was observed and the hard-sphere structure factor was used to account for the structure factor contribution to the scattering. The interaction radius for the hard-sphere structure factor was fixed to the micelle radius. The SANS curves along with the fits are shown in Figure 1 and the fitted value for the radius are detailed in Table S6.

Table S6: Radius (in Å) from the uniform sphere fits to the SANS data shown in Figure 1 for different concentrations of DTAB, TTAB and CTAB in 1pTSA:1ChCl DES, 1pTSA:1ChCl:3W DES and 2pTSA:1ChCl:3W DES.

conc	DTAB	TTAB	CTAB
	1pTSA:1ChCl		
2 wt%	7.6 ± 0.7	9.6 ± 0.5	13.7 ± 0.5
5 wt%	9.1 ± 0.3	12.3 ± 0.1	16.7 ± 0.1
10 wt%	10.6 ± 0.1	14.4 ± 0.1	17.7 ± 0.0
	1pTSA:1ChCl:3W		
2 wt%	8.5 ± 0.7	14.5 ± 0.3	19.2 ± 0.5
5 wt%	12.0 ± 0.2	15.7 ± 0.1	19.8 ± 0.3
10 wt%	13.6 ± 0.1	16.6 ± 0.1	20.3 ± 0.2
	2pTSA:1ChCl:3W		
2 wt%	8.0 ± 0.5	9.5 ± 0.3	12.7 ± 0.3
5 wt%	8.9 ± 0.2	11.4 ± 0.1	15.0 ± 0.1
10 wt%	9.8 ± 0.1	12.9 ± 0.1	16.6 ± 0.1

S5.2 Contrast variation studies of CnTAB in DES

To get details of the micellar structures contrast variation SANS studies were done for 5 wt% CnTAB in the three DES. SANS was measured from d-CnTAB in HHH DES, h-CnTAB in DDD DES, d-Cn h-TAB in HHH DES and d-CnTAB in HDD DES. For CTAB, the d-Cn h-TAB in HHH DES contrast was not measured as the d-C16 h-TAB was contaminated. However, the structural information that was obtained from DTAB and TTAB was extended and verified for CTAB by fitting the other contrasts using constraints for the model informed by the fits for DTAB and TTAB.

The SANS from d-CnTAB in HHH DES, h-CnTAB in DDD DES and d-Cn h-TAB in HHH DES can be used to obtain broad structural information about the micellar structure. The data were initially fitted to uniform spherical model and it was not possible to fit the three contrasts to a single radius, e.g. for DTAB in 1pTSA:1ChCl DES the spherical model cofitting for d-DTAB in HHH DES and h-DTAB in DDD DES gave a radius of 10.3 ± 0.1 Å, however the d-D h-TAB gave a radius of 8.0 ± 0.1 Å. Given that the underlying structure is the same for the three contrasts, this does not make physical sense but indicates that where depending on the contrast different features of the structure are visible and therefore, a core-shell variant of the spherical form factor may be applicable. The SANS data sets from d-CnTAB in HHH DES, h-CnTAB in DDD DES and d-Cn h-TAB in HHH DES were co-fitted to a core-shell spherical form factor, with a hard-sphere structure factor for the data sets where interparticle interactions were observed (5 wt% CTAB and 10 wt% CnTAB in all three DES). Both the core-radius and the shell thickness were constrained between the 3 contrasts and the shell SLD was allowed to vary to account for solvent penetration. Figure S4 shows the fits using the two models, uniform sphere and core-shell sphere, for DTAB in 1pTSA:1ChCl at the three contrasts. It can be seen from the fits that uniform spherical model with a single radius for the three contrast does not accurately describe the data, however, the core-shell spherical model where the radius and shell thickness is constraint between the three contrasts can provide good fits to the data and this was used for the different tail CnTABs in the three DES to obtain the micellar structure.

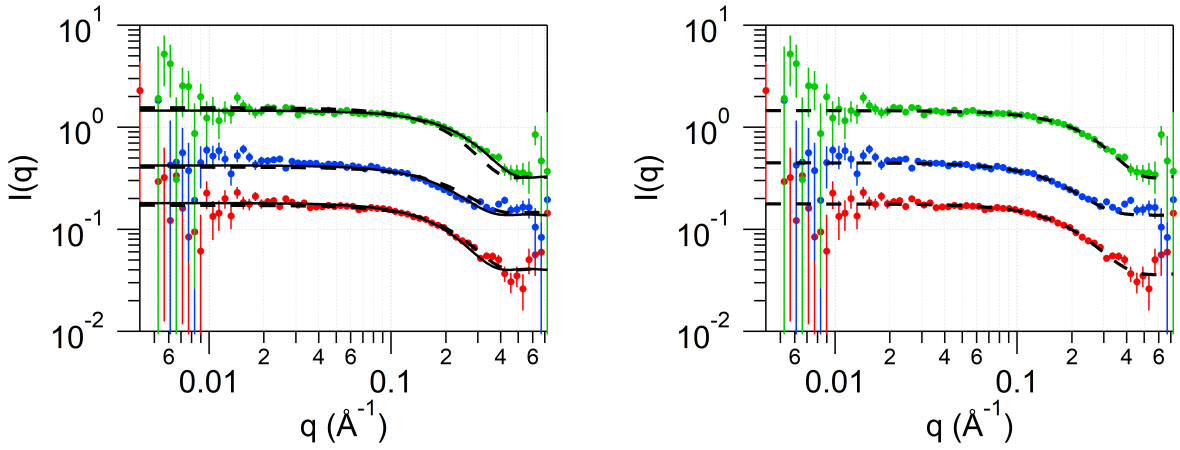

Figure S4: SANS data from 5 wt% DTAB in 1pTSA:1ChCl at three contrasts: d-DTAB in HHH DES (red), h-DTAB in DDD DES (blue) and d-D h-TAB in HHH DES (green). (a) The data fitted to the uniform sphere model with the radius allowed to vary between the three contrasts (solid black line) and co-fitted with the same radius for the 3 contrasts (dashed black line). (b) The data co-fitted to the core-shell sphere model with the same radius and thickness between for the three contrasts (dashed black line). The SANS patterns are offset along the y-axis for clarity

The fit parameters along with the error estimates for the different CnTABs in the three DES are given in Table S7. For the CTAB data set, where only two contrasts were available, the shell thickness was fixed to the average value obtained from DTAB and TTAB (as no systematical variation of the shell thickness was observed with the solvent or the CnTAB chain length) and radius and the SLD of the shell was fitted between two contrasts. Using the fitted values of shell SLD, the volume fraction of the solvent in the shell was calculated using the SLD of the tail and the SLD of the solvent ($\phi_{solvent} \times SLD_{solvent} + (1 - \phi_{solvent}) \times SLD_{tail} = SLD_{shell}$) at that contrast and found to be rather high at ∼80%.

Table S7: Spherical core-shell fit parameters for the d-CnTAB in HHH DES, h-CnTAB in DDD DES and d-Cn h-TAB in HHH DES for the 3 DES: 1pTSA:1ChCl, 1pTSA:1ChCl:3W and 2pTSA:1ChCl:3W.

Solvent	Radius (Å)	Shell Thickness (Å)	contrast	SLD shell ($\times 10^{-6}$Å^{-2})	$\phi_{solvent}$[a]
			DTAB		
110 DES	8.0±0.1	6.4±1.1	dD-dTAB in HHH DES	1.2±0.1	0.95±0.08
			hD-hTAB in DDD DES	3.8±0.4	0.84±0.09
			dD-hTAB in HHH DES	0.9±0.1	1.00±0.11
113 DES	10.1±0.3	6.1±0.5	dD-dTAB in HHH DES	2.0±0.2	0.79±0.08
			hD-hTAB in DDD DES	2.8±0.2	0.61±0.04
			dD-hTAB in HHH DES	0.6±0.1	0.94±0.16
213 DES	7.5±0.3	4.8±0.4	dD-dTAB in HHH DES	1.4±0.3	0.92±0.20
			hD-hTAB in DDD DES	3.5±0.5	0.76±0.11
			dD-hTAB in HHH DES	0.8±0.1	0.92±0.12
			TTAB		
110 DES	11.3±0.1	4.5±0.7	dT-dTAB in HHH DES	1.6±0.2	0.89±0.11
			hT-hTAB in DDD DES	2.7±0.6	0.62±0.14
			dT-hTAB in HHH DES	0.7±0.1	0.85±0.12
113 DES	14.2±0.2	4.1±0.5	dT-dTAB in HHH DES	1.8±0.3	0.82±0.14
			hT-hTAB in DDD DES	3.8±0.3	0.79±0.06
			dT-hTAB in HHH DES	0.1±0.1	0.73±0.36
213 DES	9.5±0.1	6.2±0.1	dT-dTAB in HHH DES	1.4±0.1	0.92±0.07
			hT-hTAB in DDD DES	3.8±0.5	0.82±0.11
			dT-hTAB in HHH DES	0.9±0.2	1.00±0.22
			CTAB		
110 DES	14.6±0.2	5.7±fixed	dC-dTAB in HHH DES	2.8±0.1	0.69±0.02
			hC-hTAB in DDD DES	3.3±0.1	0.74±0.02
113 DES	17.6±0.1	5.6±fixed	dC-dTAB in HHH DES	2.5±0.1	0.72±0.03
			hC-hTAB in DDD DES	4.0±0.1	0.83±0.02
213 DES	12.8±0.1	3.5±fixed	dC-dTAB in HHH DES	2.9±0.3	0.68±0.07
			hC-hTAB in DDD DES	3.1±0.2	0.68±0.04

(a) $\phi_{solvent} = (SLD_{shell} - SLD_{tail})/(SLD_{solvent} - SLD_{tail})$.

The SANS from d-CnTAB in HHH DES, h-CnTAB in DDD DES, d-Cn h-TAB in HHH DES and d-CnTAB in HDD DES can be used to obtain detail structural information about the micellar structure. The data were initially fitted to core-shell spherical model and it was not possible to fit the four contrasts to a single radius and thickness, e.g. for DTAB in 1pTSA:1ChCl DES the core-shell model cofitting for d-DTAB in HHH DES, h-DTAB in DDD DES and d-D h-TAB in HHH DES gave a core radius of 8.0 ± 0.1 Åand a shell thickness of 6.4 ± 1.1 Å, however the d-DTAB in HDD DES gave a radius of 6.3 ± 1.8 Åand a shell thickness of 3.6 ± 1.9 Å. Again given the underlying structure is the same it does not make physical sense to get different values for the fit parameters and therefore to fit the data to a single model a core and two-shell model was used. This allows us to account for solvent penetration into the tail region. The core comprises the tails of the surfactant, the first shell region takes into account solvent penetration into the tail regions and a second shell region comprises the headgroups along with the solvent components. The fitting constraints on the parameters for the core and two-shell model cofitting to the 4 contrast SANS data is given in Table S8.

Table S8: Constraints applied on the fit parameters of the core and two shell model for cofitting the 4 contrast SANS data: d-CnTAB in HHH DES, h-CnTAB in DDD DES, d-Cn h-TAB in HHH DES and d-CnTAB in HDD DES.

Core Radius	Shell 1 Thickness	Shell 2 Thickness	Core SLD	Shell 1[a] SLD	Shell 2 SLD
Fitted	Fitted	Fitted	Fixed	Fitted	Fitted
Cofitted between the four contrasts			Tail SLD	Tail SLD to Solvent SLD	Head SLD to Solvent SLD

(a) The SLD for shell 1 was cofitted for d-CnTAB in HHH DES and d-Cn h-TAB in HHH DES.

The fits for DTAB in the three DES at all four contrasts are shown in the main manuscript in Figure 4 with the fit parameters in Table 1. The data and fits for TTAB are shown below in Figure S5 and Table S9 and for CTAB in Figure S6 and Table S10. For the CTAB data set, where only three contrasts were available, the shell 1 and shell 2 thicknesses and SLDs were constrained to tighter bounds informed from the fits from DTAB and TTAB in the DES.

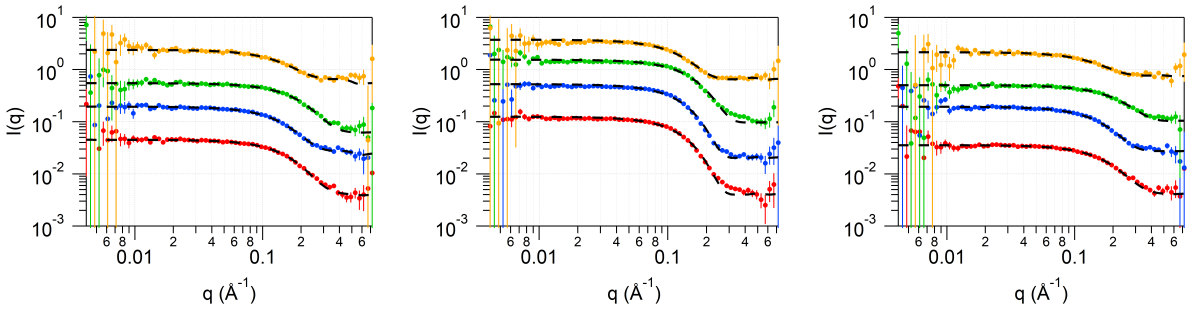

(a) (b) (c)

Figure S5: SANS data from 5 wt% TTAB in the three DES at 4 contrasts: d-TTAB in HHH DES (red), h-TTAB in DDD DES (blue), d-T h-TAB in HHH DES (green) and d-TTAB in HDD DES (orange). (a) 5 wt% CTAB in 1pTSA:1ChCl, (b) 5 wt% CTAB in 1pTSA:1ChCl:3W, and (c) 5 wt% CTAB in 2pTSA:1ChCl:3W. The data is fitted to core and two-shell model (dashed lines). The SANS patterns are offset along the y-axis for clarity.

Table S9: Core and 2 shell fit parameters for the SANS data from 5 wt% TTAB in the 3 DES co-refined for the 4 contrasts: d-TTAB in HHH DES, h-TTAB in DDD DES, d-T h-TAB in HHH DES and d-TTAB in HDD DES

	Core-Radius/Å	Shell 1 Thickness/Å	Shell 2 Thickness/Å	Shell 1 SLD /$\times 10^{-6}$ Å^{-2}	Shell 2 SLD /$\times 10^{-6}$ Å^{-2}
1pTSA:1ChCl					
d-T d-TAB in HHH DES	7.8±0.2	6.5±0.4	1.7±0.8	1.5±0.1	1.7±0.4
h-T h-TAB in DDD DES				4.7±0.1	2.7±0.9
d-T h-TAB in HHH DES				1.5±0.1	0.9±0.1
d-T d-TAB in HDD DES				2.6±0.1	4.3±0.7
1pTSA:1ChCl:3W					
d-T d-TAB in HHH DES	8.1±0.3	7.0±0.6	1.6±0.6	2.5±0.1	3.4±0.6
h-T h-TAB in DDD DES				3.0±0.1	2.3±0.6
d-T h-TAB in HHH DES				2.5±0.1	0.6±0.4
d-T d-TAB in HDD DES				3.4±0.1	5.8±0.7
2pTSA:1ChCl:3W					
d-T d-TAB in HHH DES	7.9±0.3	4.9±0.9	2.2±1	1.4±0.2	1.6±0.4
h-T h-TAB in DDD DES				3.6±0.3	3.5±0.5
d-T h-TAB in HHH DES				1.4±0.2	0.9±0.1
d-T d-TAB in HDD DES				2.3±0.1	4.5±0.9

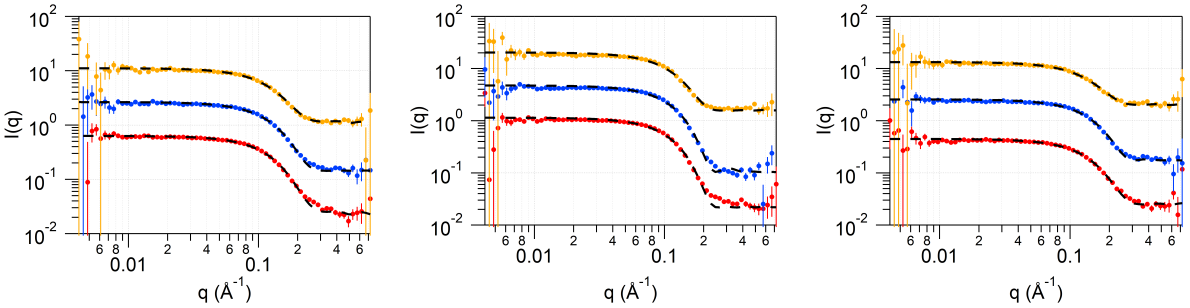

(a) (b) (c)

Figure S6: SANS data from 5 wt% CTAB in the three DES at 3 contrasts: d-CTAB in HHH DES (red), h-CTAB in DDD DES (blue) and d-CTAB in HDD DES (orange). (a) 5 wt% CTAB in 1pTSA:1ChCl, (b) 5 wt% CTAB in 1pTSA:1ChCl:3W, and (c) 5 wt% CTAB in 2pTSA:1ChCl:3W. The data is fitted to core and two-shell model (dashed lines). The SANS patterns are offset along the y-axis for clarity.

Table S10: Core and 2 shell fit parameters for the SANS data from 5 wt% CTAB in the 3 DES co-refined for the 3 contrasts: d-CTAB in HHH DES, h-CTAB in DDD DES and d-CTAB in HDD DES

	Core-Radius/Å	Shell 1 Thickness/Å	Shell 2 Thickness/Å	Shell 1 SLD /$\times 10^{-6}$ Å^{-2}	Shell 2 SLD /$\times 10^{-6}$ Å^{-2}
1pTSA:1ChCl					
d-C d-TAB in HHH DES	9.7±0.4	5.7±2.2	2.6±2.2	1.3±0.6	2.6±0.6
h-C h-TAB in DDD DES				2.8±0.4	3.2±0.4
d-C d-TAB in HDD-DES				3.0±0.4	4.2±0.5
1pTSA:1ChCl:3W					
d-C d-TAB in HHH DES	11.6±0.5	5.1±2.1	3.0±2.6	2.5±0.3	4.7±1
h-C h-TAB in DDD DES				1.2±0.7	2.0±1.0
d-C d-TAB in HDD-DES				3.9±0.1	5.6±1.3
2pTSA:1ChCl:3W					
d-C d-TAB in HHH DES	9±1.3	5.2±2.6	1.6±1.1	1.4±0.5	5.0±0.9
h-C h-TAB in DDD DES				1.7±0.9	2.5±1.2
d-C d-TAB in HDD-DES				2.8±0.5	6.5±1.8

References

[1] Nerea Rodriguez Rodriguez, Lieven Machiels, and Koen Binnemans. p-toluenesulfonic acid-based deep-eutectic solvents for solubilizing metal oxides. *ACS Sustain. Chem. Eng.*, 7(4):3940–3948, 2019.

[2] Jmol: an open-source Java viewer for chemical structures in 3D. http://www.jmol.org/.

[3] SasView for Small Angle Scattering Analysis. https://www.sasview.org/.